# High-Performance Indirect-Drive Cryogenic Implosions at High Adiabat on the National Ignition Facility

K. L. Baker,[1] C. A. Thomas,[1] D. T. Casey,[1] S. Khan,[1] B. K. Spears,[1] R. Nora,[1] T. Woods,[1] J. L. Milovich,[1] R. L. Berger,[1] D. Strozzi,[1] D. Clark,[1] M. Hohenberger,[1] O. A. Hurricane,[1] D. A. Callahan,[1] O. L. Landen,[1] B. Bachmann,[1] R. Benedetti,[1] R. Bionta,[1] P. M. Celliers,[1] D. Fittinghoff,[1] C. Goyon,[1] G. Grim,[1] R. Hatarik,[1] N. Izumi,[1] M. Gatu Johnson,[2] G. Kyrala,[3] T. Ma,[1] M. Millot,[1] S. R. Nagel,[1] A. Pak,[1] P. K. Patel,[1] D. Turnbull,[1] P. L. Volegov,[3] and C. Yeamans[1]

[1]*Lawrence Livermore National Laboratory, Livermore, California 94550, USA*

[2]*Plasma Science and Fusion Center, Massachusetts Institute of Technology, Cambridge, Massachusetts 02139, USA*

[3]*Los Alamos National Laboratory, Los Alamos, New Mexico 87545, USA*

(Received 24 January 2018; revised manuscript received 14 July 2018; published 26 September 2018)

To reach the pressures and densities required for ignition, it may be necessary to develop an approach to design that makes it easier for simulations to guide experiments. Here, we report on a new short-pulse inertial confinement fusion platform that is specifically designed to be more predictable. The platform has demonstrated $99\% + 0.5\%$ laser coupling into the hohlraum, high implosion velocity (411 km/s), high hotspot pressure ($220 + 60$ Gbar), and high cold fuel areal density compression ratio (>400), while maintaining controlled implosion symmetry, providing a promising new physics platform to study ignition physics.

DOI: 10.1103/PhysRevLett.121.135001

For indirect drive inertial confinement fusion (ICF), a spherical shell of deuterium-tritium fuel (DT) is imploded to reach fusion conditions, self-heating, and/or burn [1,2]. At the National Ignition Facility (NIF), a high-$Z$ cylindrical hohlraum is heated with 192 laser beams. The resultant x rays ionize the exterior of the spherical ablator and accelerate the remaining ablator and DT fuel inward. A diagram of an ICF target is shown in the upper left of Fig. 1. For high neutron yields, the hotspot must reach 4–5 keV and an areal density of 0.2–0.3 g/cm$^2$, which can initiate burn if the total areal density $\rho R$ of the DT is 1–2 g/cm$^2$. By design, these implosions must be near 1D, and have high in-flight kinetic energy (i.e., velocities ~380–400 km/s). Past experiments have been challenged by hydrodynamic instabilities [3], implosion symmetry [4,5], and/or laser plasma instabilities (LPI) [6,7] and models have had difficulty predicting small changes. Here, we present experiments that leverage a short laser pulse, reduced hohlraum wall motion, increased hydrodynamic stability, and high coupled energy to substantially improve predictability.

Our design, called "BigFoot," is more robust to hydrodynamic instabilities and hohlraum plasma physics and more tolerant of fuel preheat, errors in shock timing, and variations in shock strength [8]. These goals extend principles used to go from the "Low Foot" [9,10] to the "High Foot" [11–14] designs; however, we step back from these low to medium adiabat platforms [9–20], where the adiabat [2,21] of the fuel $\alpha$ is expressed as $\alpha = P/P_F$, where $P_F$ is the Fermi pressure which is related to the DT fuel density $\rho$ by $P_F[\text{Mbar}] = 2\rho^{(5/3)}$. This can also be related to the mass-averaged fuel entropy through the relation $\alpha \sim [1 + \exp((s - 0.455)/0.063)]^{0.54}$, where $s$ is the mass-averaged fuel entropy in GJ/g/keV. Low and medium adiabat designs have a low first-shock velocity in the ablator and fuel, ~18, 23, and 30 km/s for Low Foot [22], High Foot, and Diamond [20], respectively. Successive shocks are then designed to overtake the first shock near the DT ice or gas interface, leading to a longer laser pulse length. The BigFoot platform uses a short laser pulse shape, allowing the second shock to overtake the first in the ablator, near the ablator-fuel interface [8]. This sends

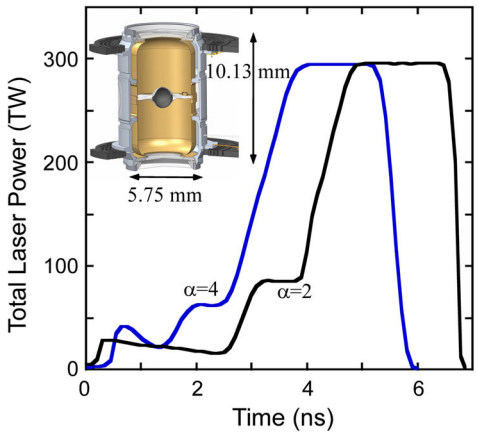


FIG. 1. Laser pulse shape comparisons for a low adiabat, $\alpha \sim 2$, HDC implosion, 140913, and the higher adiabat, $\alpha \sim 4$, BigFoot implosion, 150809.

 

a strong shock (~55 km/s) into the DT fuel, putting it on a high adiabat ($\alpha \sim 4$). The BigFoot design also uses a thin fuel layer (40 vs 70 $\mu$m) to increase velocity and reduce the capsule implosion time. These choices simplify target physics and reduce sensitivity to shock timing and fuel preheat, but limit the achievable compression and gain. However, the BigFoot platform reaches similar or higher compression than previous lower adiabat platforms. Initial BigFoot experiments also use gold hohlraums rather than uranium as oxidation is a concern for reproducibility.

The choice of high adiabat, and a short pulse, is consistent with reducing detrimental physics effects, such as hohlraum wall motion. The hohlraum wall region under the laser spots can move quickly, as temperatures can reach 2–3 keV [23]. For a long laser pulse, the wall region driven by the outer beams can expand inward and absorb the inner cones, making it impossible to achieve a symmetric implosion. To avoid this, the length of the BigFoot laser pulse is short, ~6 ns, compared to a conventional pulse (14 ns for the High Foot) [11–14]. To be compatible with this pulse, the BigFoot design utilizes a high-density carbon (HDC) ablator due to its high sound speed (fast shock transit) [17–19].

Both simulations and experiments indicate that the short pulse and high adiabat should reduce hydrodynamic instabilities relative to lower adiabat designs [24–26]. The BigFoot platform is also unique in that it is designed to have a stable (negative) fuel-ablator Atwood number, $A$, in the acceleration phase of the implosion, where $A = (\rho_f - \rho_a)/(\rho_f + \rho_a)$ [8,27]. This is accomplished by the 1–2 shock overtake in the ablator. The ablator is shock compressed 3 times and the DT fuel 2 times. Thus, the density of the ablator, $\rho_a$, is greater than the density of the fuel, $\rho_f$, throughout acceleration. Additionally, the first shock pressure is high (12 Mbar) relative to previous work with HDC (10 Mbar) [17]. Experiments operated below 12 Mbar risk being in the coexistence regime for HDC (solid and liquid phases), thereby seeding instability [17,28]. A comparison of a BigFoot pulse ($\alpha \sim 4$), and a more conventional pulse ($\alpha \sim 2$) is shown in Fig. 1 in terms of laser power $P$ vs time $t$, the main difference being the ~1 ns difference in foot duration.

The BigFoot platform is designed to reduce LPI that occurs in high gas fill hohlraums. Previous platforms used hohlraums filled with helium at densities of 0.96 to 1.6 mg/cm$^3$ to tamp the evolution of the capsule and wall blow-off. These hohlraums experience large levels of LPI, ~15%, and required multipliers on drive [29], and/or surface roughness [12], to try to account for poorly understood physics, or correlations with LPI. Other platforms used "near-vacuum" hohlraums with a gas fill density of 0.03 mg/cm$^3$ [15–19]. This choice mitigated LPI, but symmetry control and predictability were limited due to increased wall motion. The BigFoot platform introduces a gas fill of 0.30 mg/cm$^3$, and calculations using F3D [30], a three-dimensional wave propagation

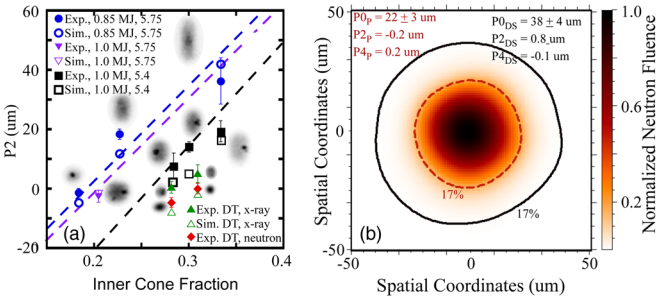


FIG. 2. (a) Hotspot images and the $P_2$ component of the core shape as a function of the inner cone fraction. The dashed blue, purple, and black lines represent the analytic model of the $P_2$ component of the core shape $a_2$ in Eq. (1), for the 5.75(0.85 MJ), 5.75(1 MJ), and 5.4(1 MJ) mm diameter hohlraums, respectively, as detailed in the Supplemental Material [32]. (b) The image of the primary neutron fluence, 13–15 MeV, from 170109. The 17% of maximum contour for the primary neutron image is represented by the dashed brown line. The black contour line represents the 17% of maximum for the downscattered neutron fluence, 10–12 MeV.

*code*, predict LPI will remain low until experiments approach the energy and power limits available at NIF [31]. These choices, along with pointing detailed in the Supplemental Material [32], have enabled 99% coupling.

Initial experiments used an existing hohlraum, 5.75 mm in diameter by 10.13 mm long, and HDC capsule, 844 $\mu$m inner radius, and 64 $\mu$m thick, filled with D-3He (30% $D_2$, 70% He3) at 32° K and 4073 Torr (6.7 mg/cm$^3$). In most cases, these capsules were doped with Tungsten (W) to shield the ice-ablator interface from x-ray preheat [18,19]. The W-doped capsules nominally had a 5 $\mu$m thick undoped HDC layer in the interior of the capsule, followed by a 20 $\mu$m thick W-doped HDC layer with 0.25% atomic W, and a 39 $\mu$m undoped HDC layer on the exterior of the capsule. To study symmetry and predictability, we varied the cone fraction (CF), the ratio of the peak inner beam power to the total laser power, and quantified the results by decomposing the hotspot shape into Legendre polynomials $P_l$ [40]. The results for this first set of experiments are shown in Fig. 2(a) by the solid blue circles. The first two experiments, represented by the top two solid blue circles in Fig. 2(a), used undoped HDC capsules, whereas all other experiments used W-doped capsules. All implosions utilizing W-doped capsules contained a bright region of emission in the hotspot, which we attribute to ablator material (mix) from the capsule fill tube [20].

Follow-on experiments were conducted in a 5.40 mm diameter by 10.13 mm long hohlraum, where simulations predicted a round implosion with a CF close to 0.33, maximizing the available laser power. The CF was varied in the new hohlraum, and again found to confirm the predicted hotspot shape ($P_2$) and symmetry ($P_2$ vs CF). For the 5.4 mm diameter hohlraum, the experimental results are

shown as filled black squares, and simulations by open black squares. We see good agreement between the measured hotspot shape, and the shape predicted by simulations, and find that the optimal CF in these experiments is 0.31, close to the original goal (0.33). The 5.75 mm diameter hohlraum produced a round implosion with a CF of 0.2 because the outer beams were intercepted closer to the capsule, providing more equatorial drive. To lend credence to the simplified hohlraum physics provided by the BigFoot design, the sensitivity of the hotspot second order Legendre moment $a_2$ to peak cone fraction CF and hohlraum radius can also be explained using a 2D analytic vacuum laser and x-ray transport view factor model as detailed in the Supplemental Material [2,41,42]. The results of this model are represented by the dashed lines on Fig. 2(a), which match the measured and simulated sensitivity to CF and hohlraum diameter. The model also accurately predicts the effect of the increase in the peak power duration on the shape as a function of CF as seen by the measured data points going between the solid blue circles (0.85 MJ) and the purple triangle (1 MJ).

With the conclusion of these experiments, three DT fuel layer experiments were fielded. In these experiments the hotspot emission, in terms of Legendre $P_2$, is found to be $\sim 9(14)$ $\mu$m more oblate than a gas-fill implosion at the same CF for the x-ray emission, filled green triangles (neutron emission, solid red triangles) in Fig. 2(a). Simulations indicate this is due to the increased mass of the DT ice layer, and a delay in the trajectory of the implosion. This series concluded on 170109, which was inferred to have a near-1D hotspot [see Fig. 2(b)], an inferred velocity of $411 \pm 20$ km/s, and a neutron $P_2$ of $-0.2$ $\mu$m. As seen in Fig. 2(b), the downscatter neutron image is also symmetric, $P_2 < 1$ $\mu$m. The overall performance in this experiment was higher than *all* previous implosions at similar power, energy, and scale. The hotspot pressure for the three DT implosions increased monotonically with laser energy $E$ as shown in Fig. 3 by the green

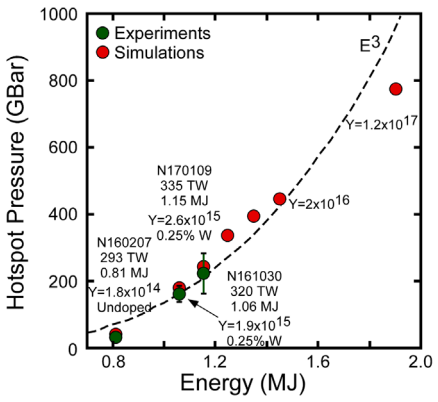


FIG. 3. Hotspot pressure as a function of laser energy. The experimental data are represented by the green circles, and the simulated hotspot pressures by the red circles.

circles, and indicate a hot spot pressure scaling as $E^3$ using techniques detailed in Ref. [11]. These results are consistent with the hotspot pressure scaling expected from 0D analytic models of the implosion, as detailed in the Supplemental Material [32], and provide additional indications that the platform is behaving according to analytic models. The first DT experiment, 160207, was conducted in a 5.75 mm diameter hohlraum with an undoped HDC ablator. Importantly, the down-scattered ratio, or DSR, in this experiment (0.014) utilizing an undoped HDC capsule was 36% below simulations (0.022), even though calculations reproduce the observed shape and time of peak emission. The down-scattered ratio, or DSR, is given by the ratio of the number of neutrons at 10–12 MeV to the number of neutrons at 13–15 MeV, and is proportional to the compressed fuel + hot spot areal density, which causes the scattering of high energy neutrons. The latter two layered DT shots in the 5.40 mm diameter hohlraums used HDC ablators with a 0.25% W dopant layer and the measured DSR was much higher (0.029), suggesting that capsule dopant could be critical to producing a DSR close to simulation (0.032). The discrepancy in the first experiment (160207) could be consistent with enhanced instability at the ice-ablator interface [43], or, interface physics missing from simulations. Historically, most experiments have measured a DSR less than predicted [43–45]. These results suggest that other platforms could benefit from testing the sensitivity of DSR to capsule dopant level.

To put these results in context, a number of simulations were run for comparison to data, as well as make predictions at increased laser energy. As shown (Fig. 3), these simulations also follow the $E^3$ hotspot scaling. Since these targets were not designed to absorb such high energies, the final simulation point at 1.9 MJ scaled the capsule thickness and DT layer thickness by 20% to enable sufficient remaining mass in the ablator. The 20% thicker DT layer resulted in a DSR that was ~15% higher than the low energy simulations. This illustrates one way in which high adiabat implosions can achieve higher DT areal densities. According to simulations, which may not hold at the higher energies, high adiabat platforms could in principle reach and exceed several of the elusive milestones associated with ICF including hotspot ignition [46] ($Y > 1 \times 10^{16}$), capsule gain exceeding unity ($Y > 6 \times 10^{16}$, fusion yield exceeds energy absorbed by the capsule), and possibly even ignition [47] ($Y > 1 \times 10^{17}$, alpha heating exceeds all losses). Although the simulation at 1.9 MJ indicates this target is igniting, we point out that the yield is limited by the low DT fuel areal density, DSR = 3.5%. To reach high gains, $Y \gg 10^{18}$, without more laser energy would require a higher compression ratio and areal density than achieved with BigFoot or with previous or existing lower adiabat platforms.

Table I provides a comparison of the two W-doped BigFoot layered DT shots, 161030 and 170109, with two of

TABLE I. Summary of experimentally measured and inferred performance parameters from the BigFoot and High Foot DT ice layered implosions with high hotspot pressure.

| | N161030 | N170109 | N140520 | N150121 |
|---|---|---|---|---|
| Hohlraum size (mm) | 5.4 by 10.13 | 5.4 by 10.13 | 5.75 by 9.43 | 5.75 by 9.43 |
| Peak power (TW) | 320 | 335 | 391 | 390 |
| Laser energy (MJ) | 1.06 | 1.15 | 1.76 | 1.74 |
| Initial DT ice layer thickness ($\mu$m) | 40.4 | 41.0 | 69.3 | 69.4 |
| Inner radius ($\mu$m) | 844 | 844 | 948 | 948 |
| Ablator thickness ($\mu$m) | 63.8 (HDC) | 65.3 (HDC) | 177 (CH) | 177 (CH) |
| DSR (%) | $2.86 \pm 0.24$ | $2.86 \pm 0.13$ | $4.08 \pm 0.2$ | $4.02 \pm 0.18$ |
| DT yield (13 to 15 MeV) | $1.67 \times 10^{15} \pm 1.7\%$ Sim. $2.26 \times 10^{15}$ | $2.33 \times 10^{15} \pm 3.8\%$ Sim. $4.07 \times 10^{15}$ | $7.6 \times 10^{15} \pm 1.8\%$ | $6.2 \times 10^{15} \pm 2.2\%$ |
| Tion (keV) | $4.13 \pm 0.12$ | $4.16 \pm 0.12$ | $5.54 \pm 0.15$ | $5.21 \pm 0.11$ |
| $\tau_{\text{gamma-rayburn width}}$ (ps) | $138 \pm 22$ | $135 \pm 22$ | $145 \pm 21$ | $131 \pm 30$ |
| Primary radius ($\mu$m)—17% | $24.2 \pm 2.4$ | $22 \pm 2.7$ | $27.6 \pm 2.2$ | $27.1 \pm 2.2$ |
| Secondary radius ($\mu$m)—17% | $33.3 \pm 3.6$ | $38.0 \pm 3.8$ | $42.6 \pm 1.3$ | $43.3 \pm 1.4$ |
| Areal density of cold fuel (g/cm$^2$) | $0.43 \pm 0.04$ | $0.41 \pm 0.05$ | $0.65 \pm 0.05$ | $0.63 \pm 0.04$ |
| Cold fuel compression ratio | $421 \pm 40$ | $388 \pm 48$ | $376 \pm 28$ | $356 \pm 23$ |
| Implosion velocity (km/s) | $390 \pm 19$ | $411 \pm 20$ | $367 \pm 15$ | $377 \pm 15$ |
| Convergence ratio | $26 \pm 3.9$ | $22 \pm 3.3$ | $22 \pm 3.3$ | $22 \pm 3.3$ |
| Hotspot areal density (g/cm$^2$) | $0.12 \pm 0.02$ | $0.15 \pm 0.05$ | $0.14 \pm 0.04$ | $0.15 \pm 0.03$ |
| Hotspot pressure (GBar) | $161 \pm 21$ | $220 \pm 60$ | $218 \pm 51$ | $219 \pm 39$ |
| Hotspot energy (J) | $1431 \pm 334$ | $1473 \pm 644$ | $2991 \pm 940$ | $2912 \pm 891$ |

the highest performing High Foot experiments using the analysis in Ref. [11]. The convergence ratio is defined as the ratio of the initial inner radius of the ablator to the radius of the down-scattered neutron image, and the cold fuel compression ratio is defined as the ratio of the $\rho R$ of the compressed fuel, 19.3*DSR-$\rho R_{HS}$, to the $\rho R$ of the initial DT ice (initial density 0.255 g/cm$^3$) [11]. Since BigFoot experiments are high adiabat ($\alpha = 4$), and have significantly less DT ice than most experiments, 41 vs 69 $\mu$m, one should expect the areal density for BigFoot experiments to be substantially less than $41/69 = 0.6$x the High Foot; Table I shows this is not the case. Moreover, quantities that should be independent of the initial DT fuel thickness, namely, convergence ratio, cold fuel compression ratio (~22), hotspot areal density (~0.15 g/cm$^2$), and hotspot pressure (~220 Gbar) are very comparable. This may indicate that BigFoot implosions are more similar to simulations, and can be used to identify factors important to compression. As an example, the results herein suggest experiments using the High Foot target and laser pulse could benefit from testing the sensitivity of DSR to the capsule dopant level.

In summary, a new ICF platform has demonstrated control of implosion symmetry, a neutron $P_2$ of $-0.2$ $\mu$m, and high implosion performance (~220 Gbar) at modest laser energy (1.15 MJ) on the NIF for a target at high DT adiabat (4). These advances are attributed to the laser pulse length (6 ns), high DT adiabat, stable Atwood number, high density ablator and first shock strength (12 Mbar), hohlraum gas fill (0.3 mg/cm$^3$), and unique laser pointing as detailed in the Supplemental Material [32]. Though these features are *conservative* and expected to reduce performance, the benefit is that they reduce hohlraum wall motion, hydrodynamic instabilities, LPI and improve predictability to simplify future physics studies. Upcoming experiments will test the effects of physical scale and adiabat, and see if changes to the target (e.g., a hohlraum foam liner [48]) can further improve control.

We wish to thank the NIF operations team. This work was performed under the auspices of the U.S. Department of Energy by Lawrence Livermore National Laboratory under Contract No. DE-AC52-07NA27344.

[1] S. Atzeni and J. Meyer-ter-Vehn, *The Physics of Inertial Fusion* (Oxford Science Press, Oxford, 2004).
[2] J. Lindl, Development of the indirect-drive approach to inertial confinement fusion, and the target physics basis for ignition, and gain, Phys. Plasmas **2**, 3933 (1995).
[3] D. S. Clark, C. R. Weber, J. L. Milovich, J. D. Salmonson, A. L. Kritcher, S. W. Haan, B. A. Hammel, D. E. Hinkel, O. A. Hurricane, O. S. Jones, M. M. Marinak, P. K. Patel, H. F. Robey, S. M. Sepke, and M. J. Edwards, Three-dimensional simulations of low foot and high foot implosion experiments on the National Ignition Facility, Phys. Plasmas **23**, 056302 (2016).
[4] G. A. Kyrala *et al.*, Symmetry tuning for ignition capsules via the symcap technique, Phys. Plasmas **18**, 056307 (2011).
[5] R. P. J. Town *et al.*, Dynamic symmetry of indirectly driven inertial confinement fusion capsules on the National Ignition Facility, Phys. Plasmas **21**, 056313 (2014).

[6] O. S. Jones *et al.*, Towards a more universal understanding of radiation drive in gas-filled hohlraums, J. Phys. Conf. Ser. **717**, 012026 (2016).
[7] P. Michel, S. H. Glenzer, L. Divol, D. K. Bradley, D. Callahan, S. Dixit, S. Glenn, D. Hinkel, R. K. Kirkwood, J. L. Kline, W. L. Kruer, G. A. Kyrala, S. Le Pape, N. B. Meezan, R. Town, K. Widmann, E. A. Williams, B. J. MacGowan, J. Lindl, and L. J. Suter, Symmetry tuning via controlled crossed-beam energy transfer on the National Ignition Facility, Phys. Plasmas **17**, 056305 (2010).
[8] C. Thomas, BigFoot, a program to reduce risk for indirect drive laser fusion, Bull. Am. Phys. Soc. **61**, 224 (2016); http://meetings.aps.org/link/BAPS.2016.DPP.NI2.6.
[9] M. J. Edwards, P. K. Patel, J. D. Lindl, L. J. Atherton, S. H. Glenzer *et al.*, Progress towards ignition on the National Ignition Facility, Phys. Plasmas **20**, 070501 (2013).
[10] J. D. Lindl *et al.*, Review of the national ignition campaign 2009–2012 (vol. 21, 020501, 2014), Phys. Plasmas **21**, 129902 (2014).
[11] O. A. Hurricane, D. A. Callahan, D. T. Casey, P. M. Celliers, C. Cerjan, E. L. Dewald, T. R. Dittrich, T. Doeppner, D. E. Hinkel, L. F. Berzak Hopkins, J. L. Kline, S. Le Pape, T. Ma, A. G. MacPhee, J. L. Milovich, A. Pak, H.-S. Park, P. K. Patel, B. A. Remington, J. D. Salmonson *et al.*, Fuel gain exceeding unity in an inertially confined fusion implosion, Nature (London) **506**, 343 (2014).
[12] O. A. Hurricane *et al.*, The high-foot implosion campaign on the National Ignition Facility, Phys. Plasmas **21**, 056314 (2014).
[13] H.-S. Park, O. A. Hurricane, D. A. Callahan, D. T. Casey, E. L. Dewald, T. R. Dittrich, T. Döppner, D. E. Hinkel, L. F. Berzak Hopkins, S. Le Pape, T. Ma, P. K. Patel, B. A. Remington, H. F. Robey, J. D. Salmonson, and J. L. Kline, High-Adiabat High-Foot Inertial Confinement Fusion Implosion Experiments on the National Ignition Facility, Phys. Rev. Lett. **112**, 055001 (2014).
[14] T. R. Dittrich, O. A. Hurricane, D. A. Callahan, E. L. Dewald, T. Döppner, D. E. Hinkel, L. F. Berzak Hopkins, S. Le Pape, T. Ma, J. L. Milovich, J. C. Moreno, P. K. Patel, H.-S. Park, B. A. Remington, J. D. Salmonson, and J. L. Kline, Design of a High-Foot High-Adiabat ICF Capsule for the National Ignition Facility, Phys. Rev. Lett. **112**, 055002 (2014).
[15] L. F. Berzak Hopkins *et al.*, First High-Convergence Cryogenic Implosion in a Near-Vacuum Hohlraum, Phys. Rev. Lett. **114**, 175001 (2015).
[16] N. B. Meezan *et al.*, Cryogenic tritium-hydrogen-deuterium and deuterium-tritium layer implosions with high density carbon ablators in near-vacuum hohlraums, Phys. Plasmas **22**, 062703 (2015).
[17] A. J. MacKinnon *et al.*, High-density carbon ablator experiments on the National Ignition Facility, Phys. Plasmas **21**, 056318 (2014).
[18] D. D. Ho, Ignition capsule design with a high-density carbon (HDC) ablator for the national ignition facility (NIF), Bull. Am. Phys. Soc. **52**, 2 (2007).
[19] D. D.-M. Ho, S. W. Haan, J. D. Salmonson, D. S. Clark, J. D. Lindl, J. L. Milovich, C. A. Thomas, L. F. Berzak Hopkins, and N. B. Meezan, Implosion configurations for robust ignition using high- density carbon (diamond) ablator for indirect-drive ICF at the National Ignition Facility, J. Phys. Conf. Ser. **717**, 012023 (2016).
[20] L. Divol *et al.*, Symmetry control of an indirectly driven high-density-carbon implosion at high convergence and high velocity, Phys. Plasmas **24**, 056309 (2017).
[21] S. W. Haan *et al.*, Point design targets, specifications, and requirements for the 2010 ignition campaign on the National Ignition Facility, Phys. Plasmas **18**, 051001 (2011).
[22] K. L. Baker *et al.*, Adiabat-shaping in indirect drive inertial confinement fusion, Phys. Plasmas **22**, 052702 (2015).
[23] J. E. Ralph, O. Landen, L. Divol, A. Pak, T. Ma, D. A. Callahan, A. Kritcher, T. Döppner, D. E. Hinkel, C. Jarrott, J. D. Moody, B. B. Pollock, O. Hurricane, and M. J. Edwards, The Influence of Hohlraum Dynamics on Implosion Symmetry in Indirect Drive Inertial Confinement Fusion Experiments Phys. Plasmas **25**, 082701 (2018).
[24] D. T. Casey *et al.*, Reduced instability growth with high-adiabat high-foot implosions at the National Ignition Facility, Phys. Rev. E **90**, 011102(R) (2014).
[25] J. L. Peterson, D. T. Casey, O. A. Hurricane, K. S. Raman, H. F. Robey, and V. A. Smalyuk, Validating hydrodynamic growth in National Ignition Facility implosions, Phys. Plasmas **22**, 056309 (2015).
[26] V. A. Smalyuk, C. R. Weber, H. F. Robey, D. T. Casey, K.-C. Chen, D. S. Clark, M. Farrell, S. Felker, J. E. Field, S. W. Haan, B. A. Hammel, A. V. Hamza, D. Hoover, J. J. Kroll, O. L. Landen, A. G. MacPhee, D. Martinez, A. Nikroo, and N. Rice, Hydrodynamic instability growth of three-dimensional modulations in radiation-driven implosions with "low-foot" and "high-foot" drives at the National Ignition Facility, Phys. Plasmas **24**, 042706 (2017).
[27] D. S. Clark, A. L. Kritcher, S. A. Yi, A. B. Zylstra, S. W. Haan, and C. R. Weber, Capsule physics comparison of National Ignition Facility implosion designs using plastic, high density carbon, and beryllium ablators, Phys. Plasmas **25**, 032703 (2018).
[28] D. G. Hicks, T. R. Boehly, P. M. Celliers, D. K. Bradley, J. H. Eggert, R. S. McWilliams, R. Jeanloz, and G. W. Collins, High-precision measurements of the diamond Hugoniot in and above the melt region, Phys. Rev. B **78**, 174102 (2008).
[29] O. S. Jones *et al.*, A high-resolution integrated model of the National Ignition Campaign cryogenic layered experiments, Phys. Plasmas **19**, 056315 (2012).
[30] R. L. Berger, B. F. Lasinski, T. B. Kaiser, E. A. Williams, A. B. Langdon, and B. I. Cohen, Theory and three-dimensional simulation of light filamentation in laser-produced plasma, Phys. Fluids B **5**, 2243 (1993).
[31] Richard Berger, K. L. Baker, C. A. Thomas, J. L. Milovich, A. B. Langdon, D. J. Strozzi, and M. Michel, Lowering the risk of stimulated Brillouin backscatter from NIF hohlraums by re-pointing beams, Bull. Am. Phys. Soc. **60**, 137 (2015); http://meetings.aps.org/link/BAPS.2015.DPP.JO5.13.
[32] See Supplemental Material at http://link.aps.org/supplemental/10.1103/PhysRevLett.121.135001 for detailed information regarding cone and quad splitting pointing in the BigFoot platform, additional benefits of the shorter laser pulse shape, details of the analytic shape model and the analytic scaling of hotspot pressure with laser energy which includes Refs. [33–39].

[33] R. L. Berger, Stimulated Brillouin scattering in inhomogeneous flowing plasma, Phys. Fluids **27**, 1796 (1984).
[34] M. B. Schneider *et al.*, Images of the laser entrance hole from the static x-ray imager at NIF, Rev. Sci. Instrum. **81**, 10E538 (2010).
[35] J. Lindl, P. Amendt, R. L. Berger, S. Gail Glendinning, S. H. Glenzer, S. W. Haan, R. L. Kauffman, O. L. Landen, and L. J. Suter, The physics basis for ignition using indirect-drive targets on the National Ignition Facility, Phys. Plasmas **11**, 339 (2004).
[36] O. A. Hurricane, A. Kritcher, D. A. Callahan, O. Landen *et al.*, On the importance of minimizing "coast-time" in x-ray driven inertially confined fusion implosions, Phys. Plasmas **24**, 092706 (2017).
[37] Y. Saillard, Acceleration, and deceleration model of indirect drive ICF capsules, Nucl. Fusion **46**, 1017 (2006).
[38] A. Casner, T. Jalinaud, L. Masse, and D. Galmiche, Convergent ablation measurements of plastic ablators in gas-filled rugby hohlraums on OMEGA, Phys. Plasmas **22**, 100702 (2015).
[39] A. Kemp, J. Meyer-ter-Vehn, and S. Atzeni, Stagnation Pressure of Imploding Shells and Ignition Energy Scaling of Inertial Confinement Fusion Targets, Phys. Rev. Lett. **86**, 3336 (2001).
[40] J. R. Rygg, O. S. Jones, J. E. Field, M. A. Barrios, L. R. Benedetti, G. W. Collins, D. C. Eder, M. J. Edwards, J. L. Kline, J. J. Kroll, O. L. Landen, T. Ma, A. Pak, J. L. Peterson, K. Raman, R. P. J. Town, and D. K. Bradley, 2D X-Ray Radiography of Imploding Capsules at the National Ignition Facility, Phys. Rev. Lett. **112**, 195001 (2014).
[41] O. L. Landen, P. A. Amendt, L. J. Suter, R. E. Turner, S. G. Glendinning, S. W. Haan, S. M. Pollaine, B. A. Hammel, M. Tabak, M. D. Rosen, and J. D. Lindl, A simple time-dependent analytic model of the P2 asymmetry in cylindrical hohlraums, Phys. Plasmas **6**, 2137 (1999).
[42] D. Turnbull, L. F. Berzak Hopkins, S. Le Pape, L. Divol, N. Meezan, O. L. Landen, D. D. Ho, A. Mackinnon, A. B. Zylstra, H. G. Rinderknecht, H. Sio, R. D. Petrasso, J. S. Ross, S. Khan, A. Pak, E. L. Dewald, D. A. Callahan, O. Hurricane, W. W. Hsing, and M. J. Edwards, Symmetry control in subscale near-vacuum hohlraums, Phys. Plasmas **23**, 052710 (2016).
[43] C. R. Weber, L. F. Berzak Hopkins, D. S. Clark, T. Döppner, S. W. Haan, D. D. Ho, N. B. Meezan, J. L. Milovich, H. F. Robey, and V. A. Smalyuk, Modeling and measuring fuel-ablator interface mixing in inertial-confinement fusion implosions, *The 15th International Workshop on the Physics of Compressible Turbulent Mixing, University of Sydney, Australia, 2016* (2016), https://pdfs.semanticscholar.org/a9d9/69c447dd67a54de97d1b9e0b2108b05a9c59.pdf.
[44] D. S. Clark, A. L. Kritcher, J. L. Milovich, J. D. Salmonson, C. R. Weber, S. W. Haan, B. A. Hammel, D. E. Hinkel, M. M. Marinak, M. V. Patel, and S. M. Sepke, Capsule modeling of high foot implosion experiments on the National Ignition Facility, Plasma Phys. Controlled Fusion **59**, 055006 (2017).
[45] N. B. Meezan *et al.*, Cryogenic THD and DT layer implosions with high density carbon ablators in near-vacuum hohlraums, Phys. Plasmas **22**, 062703 (2015).
[46] A. R. Christopherson and R. Betti, Definition of Ignition in Inertial Confinement Fusion, Bull. Am. Phys. Soc. **62**, 415 (2017); http://meetings.aps.org/link/BAPS.2017.DPP.YO7.15.
[47] R. Betti, P. Y. Chang, B. K. Spears, K. S. Anderson, J. Edwards, M. Fatenejad, J. D. Lindl, R. L. McCrory, R. Nora, and D. Shvarts, Thermonuclear ignition in inertial confinement fusion and comparison with magnetic confinement, Phys. Plasmas **17**, 058102 (2010).
[48] K. Baker, C. Thomas, T. Baumann, R. Berger, M. Biener, D. Callahan, P. Celliers, F. Elsner, S. Felker, A. Hamza, D. Hinkel, H. Huang, O. Jones, N. Landen, J. Milovich, J. Moody, A. Nikroo, R. Olson, and D. Strozzi, In Pursuit of a More Ideal Hohlraum, Bull. Am. Phys. Soc. **60**, 322 (2015); http://meetings.aps.org/link/BAPS.2015.DPP.UO7.3.